Temporal and Spatial Monitoring and Prediction of Epidemic Outbreaks

Amin Zamiri, Hadi Sadoghi Yazdi, and Sepideh Afkhami Goli

***Abstract*—This paper introduces a nonlinear dynamic model to study spatial and temporal dynamics of epidemics of susceptible-infected-removed type. It involves modeling the respective collections of epidemic states and syndromic observations as random finite sets. Each epidemic state consists of the number of infected individuals in an isolated population system and the corresponding partially known parameters of the epidemic model. The infectious disease could spread between population systems with known probabilities based on prior knowledge of ecological and biological features of the environment. The problem is then formulated in the context of Bayesian framework and estimated via a probability hypothesis density filter. Each population system under surveillance is assumed to be homogenous and fixed, with daily reports on the number of infected people available for monitoring and prediction. When model parameters are partially known, results of numerical studies indicate that the proposed approach can help early prediction of the epidemic in terms of peak and duration.**

***Index Terms*—Filtering, nonlinear dynamic systems, spatiotemporal phenomena, syndromic surveillance.**

I. Introduction

An epidemic is a term used in epidemiology that refers to "the appearance of new cases of a particular disease in a given human population, during a given time period, at a rate that substantially exceeds the expected number based on recent experience" [1]. The effects of an epidemic can quickly spread from a region to a country, or even a group of countries [2] ranging from a local cluster of a communicable disease to a global threat, as in the case of the ongoing epidemics of AIDS, tuberculosis, and the recent outbreaks of avian influenza (H5N1), SARS, and H1N1 (swine flu) [3], [4].

In surveillance terms, "syndromic" or "prediagnosis" relates to a specific set of symptoms not requiring laboratory confirmation for diagnosis. While syndromic observations are available much earlier than that of postdiagnosis reports, they are not deterministic and suffer from noisy and incomplete data [5]–[7]. The goal of syndromic surveillance is estimating and predicting any increase in the rate of reported cases, allowing a timelier public health response [8], [9].

Manuscript received September 20, 2013; revised June 24, 2014; accepted July 7, 2014. Date of publication August 6, 2014; date of current version March 2, 2015.

A. Zamiri is with the Department of Computer Engineering, Ferdowsi University of Mashhad, Mashhad 9177948974, Iran (e-mail: amin.zamiri@gmail.com).

H. S. Yazdi is with the Department of Computer Engineering and also with the Center of Excellence on Soft Computing and Intelligent Information Processing, Ferdowsi University of Mashhad, Mashhad 9177948974, Iran (e-mail: h-sadoghi@um.ac.ir).

S. A. Goli is with the Department of Electrical and Computer Engineering, Calgary University, Alberta, Canada (e-mail: sepideh.afkhamigoli@ucalgary.ca).

Digital Object Identifier 10.1109/JBHI.2014.2338213

Syndromic surveillance algorithms and its applications have recently attracted significant attention by scientific community and the governments [8] and there is a plethora of literature devoted to this topic (more comprehensive reviews are provided in [10]–[12] and references therein).

Generally, the problem is often formulated as prospective evaluation of a single-time series. Unfortunately there is not an extensive body of the literature focusing on analysis of multiple data sources with spatial information [13]. A straightforward approach to incorporate spatial information is to apply a separate single-time series approach within each spatial region. In practice, however, the different time series under study may be influenced by common confounding factors, and so they are likely to be correlated [14]. For example, an infectious agent in one region could spread to neighboring areas through various forms of transition pathways, with similar peak and duration [15].

In this paper, a recursive information fusion algorithm is presented for the prediction of epidemic progress amongst a set of isolated population systems. These population systems could represent a specific geographical area such as a city or a country. The population dynamics within each area is described independently, with additional terms accounting for the probability of spread. The problem is then formulated in the Bayesian context of nonlinear multitarget filtering and estimated using a probability hypothesis density (PHD) filter with particle systems implementation known as particle-PHD or sequential Monte Carlo (SMC) PHD filter in tracking literature. While the Bayesian formulation and the nonlinear filtering implementation have been considered earlier, see [16]–[18], none has considered the case of spatial spread of the disease. This paper introduces a novel multitarget approach to include spatial information of reported cases while providing temporal estimates of epidemic peak and duration. We formulate and solve the optimal Bayes predictor when there are several sources of syndromic data streams (each from a specific area) and the number of outbreaks is unknown. The observation data in this case could be noisy and missed in some short intervals, as typically in the case of syndromic data [6]. Numerical results are provided in this paper as a proof of concept using syndromic data based on a real-world epidemic in Switzerland.

The celebrated susceptible-infected-removed (SIR) model [19]–[21] is a suitable epidemiological model for our framework. The epidemic curve in the SIR model is formulated by only two parameters of the population: contact rate β and recovery time γ. With values of these parameters at hand, the number of infected people could be predicted at each time step based on the current population of infected and susceptible.

Our choice of the SIR model was driven by its widespread adaptation and relevance for the operational context of the problem, which is the short-term prediction for an emerging epidemic that is spreading rapidly. Although the attractive simplicity of the SIR model is a plus, there are some shortcomings involved. A clear downside of this model is the inability to describe any spatial aspects of infectious disease spread [22], which is addressed in the proposed approach.

II. Motivation

The analysis of infection spread through linked populations systems is of great significance [23] and attracts considerable attention; the Foot and Mouth Disease epidemic of 2001 being an important example [24]. An excellent review of the literature on spatial epidemic models can be found in [5] and [25].

Incorporating spatial information into the epidemic model is motivated by two factors. These factors could contribute to earlier and more accurate modeling during the initial stages of epidemic, and are discussed in this section.

In order to benefit from spatial information, reported data from all geographical areas of interest should be modeled in a holistic approach. This is where single time-series approaches, including single-target filtering, fall short. Spatial information in these methods, if considered at all, is usually handled by running a separate algorithm for each region. Consequently, the spatial autocorrelation is neglected [5].

A. Spatial Patterns of Spread

Spatial patterns and disease spread directions could be observed during the course of an epidemic. In European continent, for example, a west–east direction of influenza spread was observable for several years [26]. The 2003/2004 influenza season in Switzerland is a clear instance of such pattern. The first wave of the epidemic appears in the final weeks of 2003 in Geneva, Switzerland, and then, spreads to nearby cities in the following weeks [15].

Ecological and geographical features could also shape certain patterns of spatial spread. In fox rabies, for example, rivers act as barriers that holds back further spread of the disease [27].

Once an outbreak is detected, prior knowledge on patterns and directions of spread could contribute to earlier predictions for clean areas, based on their risk of contamination.

B. Behavioral Similarity of Epidemics

Because of the spatial variability of the population (contact rate and recovery time), it is hypothesized that the epidemic curves could vary from place to place and even wave to wave [28]. Therefore, an epidemic in one population system could evolve differently after spreading to another. However, the variability of this kinetic process for the same strain could be usually modeled by a limited range of parameter values [29]. Pandemic influenza cases, for example, are suggested to be latent for two days and infectious for 2.5 days [30].

III. Problem Formulation

A. Modeling Population Dynamics

According to the SIR model, the population of a system can be subdivided into three interacting groups: susceptible, infectious, and removed individuals [21], [31]. Let the number of susceptible, infectious, and removed denoted by S_L, I_L, and R_L, respectively, so that $S_L + I_L + R_L = P_L$, where P_L is the total size of the population system L. To represent an epidemic progress in time as a dynamic model, the following differential equations based on the "conservation" law for the population are derived:

$$\frac{ds_L}{dt} = -q_L \tag{1}$$

$$\frac{di_L}{dt} = q_L - \gamma_L i_L \tag{2}$$

$$r_L = 1 - s_L - i_L \tag{3}$$

where

1) $s_L = S_L/P_L$, $i_L = I_L/P_L$, and $r_L = R_L/P_L$ are the normalized compartment sizes;
2) γ_L represents the average infectious period of the disease;
3) the term $q_L(i_L, s_L)$ describes the social interactions between the individuals of population. As in the classical SIR model, we assume $q_L(i_L, s_L) = \beta_L i_L s_L$. The contact rate parameter β_L is a product $\beta_L = \rho_L \,.\, \gamma_L$, with ρ_L being the basic reproductive number, which represents the average number of new infections produced by direct contact with a single infected individual that would be expected in a population of entirely susceptible subjects.

The epidemic model parameters can be assumed to be partially known for every population as interval values, that is $\beta_L \in [\bar{\beta}, \underline{\beta}]$ and $\gamma_L \in [\bar{\gamma}, \underline{\gamma}]$ for each population system of area L under study.

B. Measurement Model

For each area L (with an ongoing epidemic) at a specific time step t, we assume

$$z_L = i_L + \omega_L \tag{4}$$

where z_L is the observable proportion (reported cases at time t) of infected population in area L. The noise term ω_L is added to simulate the randomness of real-world syndromic observations (measurements noise), which is assumed to be uncorrelated to other population systems.

The collection of all measurement for all population systems (observable proportion of infected population) at time t is denoted by

$$Z_t \triangleq \{z_{i_t}, i = 1, \ldots, N_t\} \tag{5}$$

where N_t is the total number of measurements reported at time t. The aforementioned model allows for reports on the number of cases to be missed and to include noisy or false reports. The problem is then to estimate the "true" number of infected areas and normalized number of infected i_L and susceptible s_L

at time t, together with model parameters, for each area using observations z_L of (4), collected at time t.

C. Handling Spatial Information

Modeling spatial population dynamics in humans or animals requires comprehensive ecological and biological knowledge of the pathogenesis of the infectious agent. Accurate reporting of the variables involved (including mobility range, dispersal rates, contact rates, etc.) is paramount for realistic construction of a spatial model [4], [32]. In practice, however, such information is not readily available and can be very expensive to obtain [33]. Moreover, available data primarily reflect politically defined reporting units rather than biologically relevant ecological units [27].

To avoid complications that arise from comprehensive modeling of population dynamics, our model is reduced to the basic assumption of infectious disease spread based on predefined probabilities between each pair of population systems.

IV. Proposed Approach

A. Optimal Bayesian Solution

The model (1)–(3) are given in continuous time. For a recursive algorithm, a discrete-time approximation of this model is required. The state vector for each target area is adopted as

$$x = [s \ i \ \beta \ \gamma \ L]^T \tag{6}$$

where T denotes the matrix transpose. It includes i and s for every infected area and also the imprecisely known parameters β and γ as well as the area identifier L.

The state is assumed to follow a Markov process on state space $\mathcal{X} \subseteq \mathbb{R}^{n_x}$. Let M_k be the number of ongoing epidemics detected at k, where $k = t_k/\tau$ is the discrete time index for small integration interval $\tau > 0$. Suppose that, at time $k-1$, the targets are $x_{k-1,1}, \ldots, x_{k-1,M_k} \in \mathcal{X}$. At the next time step, a subset of these targets may not exist (finished epidemics), the surviving targets evolve to their new states, and some new targets may appear (due to disease spread to new areas or spontaneous epidemic emergence). This results in new states $x_{k,1}, \ldots, x_{k,M_k} \in \mathcal{X}$.

The state vector in from of (6) includes all the required information for each target (i.e., an ongoing epidemic of SIR type for an isolated population system). Following the discussions provided in Section II, the spread of disease from one area to another, as well as the possibility of new epidemic emergence in areas under study, should also be modeled. The problem is that the state evolution model for each area cannot be processed independently. Moreover, the number of infected areas in this case is unknown and false alarms in the number of reported cases (clutter) are possible.

The random finite set (RFS) [34] approach to multitarget tracking is an emerging and promising approach to address these limitations [35], [36]. In the RFS formulation, the collection of individual targets is treated as a set-valued state, and the collection of individual observations is treated as a set-valued observation, i.e.

$$X_k = \{x_{k,1}, \ldots, x_{k,M_k}\} \in \mathcal{F}(\mathcal{X}) \tag{7}$$

$$Z_k = \{z_{k,1}, \ldots, z_{k,N_k}\} \in \mathcal{F}(\mathcal{Z}) \tag{8}$$

where $\mathcal{F}(\mathcal{X})$ and $\mathcal{F}(\mathcal{Z})$ are the respective collections of all finite subsets of $\mathcal{X}$ and $\mathcal{Z}$.

Set-valued states and set-valued observations modeling approach allows the problem of dynamically estimating multiple targets in the presence of noisy and incomplete data [34]–[37]. The problem of spatial monitoring of epidemics is then formulated as multitarget tracking and is posed as a filtering problem with multitarget state space $\mathcal{F}(\mathcal{X})$ and observation space $\mathcal{F}(\mathcal{Z})$.

The RFS that models the multitarget state, is the union of state vectors that survived from previous time step, those which have been spawned by existing targets and those which appear spontaneously, and is given by

$$X_k = \left(\bigcup_{x \in X_{k-1}} S_{k|k-1}(x) \right) \cup \left(\bigcup_{x \in X_{k-1}} B_{k|k-1}(x) \right) \cup \Gamma_k. \tag{9}$$

In the aforementioned formulation, the first term is the RFS of epidemic states at discrete time index k given the previous states X_{k-1} (survived targets). $S_{k|k-1}(x)$ can take on either $\{x_k\}$ when the epidemic continues, or $\emptyset$ when the epidemic period is passed. The second term represents the RFS of newly infected areas spawned from the previous epidemics at time step $k-1$. The last term, RFS Γ_k, accounts for spontaneous epidemic emergence in clean areas.

The multitarget measurement at time step k is modeled by the RFS

$$Z_k = K_k \cup \left(\bigcup_{x \in X_k} \Theta_k(x) \right) \tag{10}$$

where $\Theta_k(x)$ is the RFS of measurements from multitarget state X_k, and K_k is the RFS of measurements due to false reports (clutter). For a given target x_k, the term $\Theta_k(x_k)$ can take on either $\{z_k\}$ when the target is detected (there is a report available for kth day) with probability $p_{D,k}(x_k)$, or $\emptyset$ when the target is missed with probability $1 - p_{D,k}(x_k)$.

The formal Bayesian solution is given in the form of the multitarget posterior density $p(X_k|Z_{1:k})$. Based on the posterior density, our aim is to predict the progress of the epidemic across areas under study at the next time step $k+1$, using the dynamic model equations.

The multitarget Bayes filter propagates the multitarget posterior density $p_k(\cdot|Z_k)$ conditioned on the sets of observations up to time k, Z_k, with the following recursions.

Step 1–Prediction:

$$p_{k|k-1}(X_k|Z_{k-1}) = \int f_{k|k-1}(X_k|X) p_{k-1}(X|Z_k) \mu_s(dx). \tag{11}$$

Step 2–Update:

$$p_k(X_k|Z_k) = \frac{g_k(Z_k|X_k) p_{k|k-1}(X_k|Z_{k-1})}{\int g_k(Z_k|X_k) p_{k|k-1}(X_k|Z_{k-1}) \mu_s(dx)} \tag{12}$$

where the dynamic model is governed by the multitarget transition density $f_{k|k-1}(X_k|X)$ and multitarget likelihood $g_k(Z_k|X_k)$ and μ_s is an appropriate reference measure on

$\mathcal{F}(\mathcal{X})$ [38]. The randomness in the multitarget evolution and observation described by (9) and (10) are, respectively, captured in $f_{k|k-1}(\cdot|\cdot)$ and $g_k(.|.)$ [39].

The function $g_k(Z_k|X_k)$ is the joint multitarget likelihood function of observing the set of measurements, Z, given the set of target states X. The parameters for this density are the set of observations Z, the unknown set of targets X, observation noise, probability of detection P_D, false alarm P_{FA}, and clutter models [40].

The evolution of the epidemic state, by neglecting the process noise for the moment, can be written according to (1) and (2) as $\dot{x} = g(x)$ where

$$g(x) = [-\beta is\ (\beta s - \gamma)i\ 0\ 0\ 0]^T. \tag{13}$$

For a small integration interval $\tau > 0$, one could approximate the state evolution in time using the Euler method:

$$x(t+\tau) \approx x(t) + \tau g(x(t)). \tag{14}$$

The state evolution in discrete time can be expressed as

$$S_{k|k-1}(x) = \begin{bmatrix} x_k[1] - \tau x_k[3]x_k[2]x_k[1] \\ x_k[2] + \tau x_k[2](x_k[3]x_k[1] - x_k[4]) \\ x_k[3] \\ x_k[4] \\ x_k[5] \end{bmatrix} + w_k. \tag{15}$$

In this notation, $x_k[i]$ represents the *i*th component of vector x_k. Process noise w in (14) is assumed to be zero-mean white Gaussian with a diagonal covariance matrix Q of size 5×5. Its components, except the first two, are set to zero based on assumption that β and γ are constant during the epidemic.

As mentioned earlier, spatial spread is modeled by a set of predefined probabilities of transition pathways between areas. In this setting, $\beta_{k|k-1}(x)$, returns an state vector of (6) with area identifier selected based on the transition probability of area $x[5]$ to other areas $(trans(.))$, and is defined by

$$B_{k|k-1} = \begin{bmatrix} s_0 \\ 1 - s_0 \\ x_{k-1}[3] \\ x_{k-1}[4] \\ trans(x_{k-1}[5]) \end{bmatrix} + v_k \tag{16}$$

where s_0 is a small random number representing the initial population of susceptible and v_k is zero-mean white Gaussian noise with a diagonal covariance matrix $\acute{Q}$ modeling the variation in epidemic parameters in the new population system. The components of matrix $\acute{Q}$ are set to zero except the second and third components. Subroutine $trans$ generates a random number identifying an area under study, such that the area with the highest transition probability with $x_{k-1}[5]$ has a higher probability of selection.

B. Estimation With Particle-PHD Filter

The recursion (11) and (12) involves multiple integrals on the space $\mathcal{F}(\mathcal{X})$, which are computationally intractable [39]. Therefore, the multitarget Bayes filter is computationally intractable. The PHD filter [41] is an approximation that propagates the first-order statistical moment, or PHD, of the RFS of states in time [35]. Since the PHD filter operates on the single-target state space, it avoids the combinatorial problem that arises from data association. These outstanding features of the PHD filter are extremely attractive for practical problems [39]. In our study, the problem of data association is resolved by including the area identifier (L) in the state vector, because the origin of reported cases of infection is always available.

For a RFS X on $\mathcal{X}$ with probability distribution *P*, its first-order moment is nonnegative function v on $\mathcal{X}$, called the intensity or PHD [35] in tracking literature, such that for each region $S \subseteq \mathcal{X}$

$$\int |X \cap S|\, P(dX) = \int_S v(x)dx. \tag{17}$$

Hence, the total mass

$$\hat{N} = \int v(x)dx \tag{18}$$

gives the expected number of elements of X that are in S. The local maxima of the intensity v are points in $\mathcal{X}$ with the highest density of expected number of targets, and therefore, can be used to generate estimates for elements of X [39].

Let v_k and $v_{k|k-1}$ denote the respective intensities associated with the multitarget posterior density p_k and the multitarget predicted density $p_{k|k-1}$ in the recursion (11) and (12). It can be shown that the posterior intensity can be propagated in time via the PHD recursion.

Step 1– Prediction:

$$v_{k|k-1}(x) = \int p_{s,k}(\varsigma) f_{k|k-1}(x|\varsigma) v_{k|k-1}(\varsigma) d\varsigma + \int \beta_{k|k-1}(x|\varsigma) v_{k-1}(\varsigma) d\varsigma + \gamma_k(x). \tag{19}$$

Step 2– Update:

$$v_k(x) = [1 - p_{D,k}(x)]\, v_{k|k-1}(x) + \sum_{z \in Z_k} \frac{p_{D,k}(x) g_k(z|x) v_{k|k-1}(x)}{\mathcal{K}_k(z) + \int p_{D,k}(\xi) g_k(z|\xi) v_{k|k-1}(\xi) d\xi} \tag{20}$$

where $\gamma_k(x)$ is intensity of the birth RFS Γ_k, $\beta_{k|k-1}(.|\varsigma)$ is intensity of the spawn RFS $B_{k|k-1}$, $p_{s,k}(\varsigma)$ is the probability of survival with previous state ς, $p_{D,k}$ is the proability of detection, and $\mathcal{K}_k$ is the intensity of clutter RFS K_k.

Since the PHD recursion involves multiple integrals that have no closed-form solutions in general, we develop an approximate solution. Generic sequential Monte Carlo techniques have been proposed to propagate the posterior intensity in time (see [42] and references therein). In this approach, state estimates are extracted from the particles representing the posterior intensity using clustering techniques such as *k*-means or expectation

maximization [43], [44]. The k-means approach was adopted for this study.

The particle-PHD approximates the intensity of the posterior PDF $p_k(X_k|Z_k)$ by a weighted random sample. Given a sequence of measurement sets $Z_{1:k}$, the approximation at time step $k > 0$ is given as follows.

In the *initialization* step, particles are distributed across the state space according to the prior. The initial intensity function v_0 is given by

$$v_0(x) = \sum_{i=1}^{L_0} w_0^{(i)} \delta\big(x - x_0^{(i)}\big). \tag{21}$$

Here, $\delta(.)$ is the Dirac delta function and $\{x_k^i, i = 1, \dots L_k\}$ are support points or particles with associated weights $\{w_k^i, i = 1, \dots L_k\}$ constructing a random measure $\{x_k^{(i)}, w_k^{(i)}\}_{i=1}^{L_k}$, where L_k is the particle count for step k. The weights are selected based on the principle of importance sampling and are normalized such that $\sum_i w_k^i = 1$.

The particles are propagated in the *prediction* stage using the dynamic model (15) and (16). Particles are also added to allow for new epidemics representing the term Γ_k in (9). The predicted intensity function $v_{k|k-1}$ at time step k is

$$v_{k|k-1}(x) = \sum\nolimits_{i=1}^{L_{k-1}+J_k} \tilde{w}_{k|k-1}^{(i)} \delta\big(x - \tilde{x}_k^{(i)}\big) \tag{22}$$

where

$$\tilde{x}_k^{(i)} \sim \begin{cases} q_k\big(\cdot\,|x_{k-1}^{(i)}, Z_k\big), & i = 1, \dots, L_{k-1} \\ p_k\big(\cdot\,|Z_k\big), & i = L_{k-1}+1, \dots, L_{k-1}+J_k \end{cases} \tag{23}$$

and

$$\tilde{w}_{k|k-1}^{(i)} = \begin{cases} \dfrac{\phi_{k|k-1}\big(\tilde{x}_k^{(i)}, x_k^{(i)}\big)}{q_k\big(\tilde{x}_k^{(i)}|x_{k-1}^{(i)}, Z_k\big)} w_{k-1}^{(i)}, & i = 1, \dots, L_{k-1} \\ \dfrac{1}{J_k} \dfrac{\gamma_k\big(\tilde{x}_k^{(i)}\big)}{p_k\big(\tilde{x}_k^{(i)}|Z_k\big)}. & i = L_{k-1}+1, \dots, L_{k-1}+J_k \end{cases} \tag{24}$$

In the aforementioned equations q_t and p_t are two important sampling proposal densities by which the samples are obtained. Here, the L_{k-1} particles are predicted forward by the kernel $\phi_{k|k-1}$ that captures the dynamic model (14) and (16), and an additional J_k particles are drawn to detect new and emergent epidemics.

The prediction steps are carried out until a set of measurements of reported cases Z_k becomes available, at time index k. When the measurements are received, weights are calculated for the particles based on their likelihoods, which are determined by the statistical distance of the particles to the set of observations (i.e., ongoing epidemics). Given that the particle representation of the predicted intensity function is available at time step k, the *updated* intensity function v_k is given by

$$v_k(x) = \sum\nolimits_{i=1}^{L_{k-1}+J_k} \tilde{w}_k^{(i)} \delta\big(x - \tilde{x}_k^{(i)}\big). \tag{25}$$

In this formulation, $\tilde{w}_k^{(i)}$ are given by

$$\tilde{w}_k^{(i)} = \left[\big(1 - p_{D,k}\big(\tilde{x}_k^{(i)}\big)\big) + \sum_{z \in Z_k} \frac{p_{D,k}\big(\tilde{x}_k^{(i)}\big) g_k\big(z|\tilde{x}_k^{(i)}\big)}{\mathcal{K}_k(z) + C_k(z)}\right] \times \tilde{w}_{k|k-1}^{(i)} \tag{26}$$

where $C_k(z) = \sum_{j=1}^{L_{k-1}+J_k} p_{D,k}(\tilde{x}_k^{(j)}) g_k(z|\tilde{x}_k^{(j)}) \tilde{w}_{k|k-1}^{(j)}$. We, therefore, have a discrete weighted approximation of the true posterior $p_k(X_k|Z_k)$. The sum of the weights gives the estimated number of ongoing epidemics. For more details on prediction and update steps see [40] and [43] and for detailed implementation techniques including resampling step see [42].

V. Numerical Results

A. Simulation Setup

An experimental dataset based on the reported cases in 2003/2004 influenza season in Switzerland (see Section II) is used for prediction of an epidemic. Three cities Geneva, Bern, and Lausanne were chosen for the following experiments.

This choice was driven by two main factors; first there is one dominant influenza strain in the period of interest, and second clear empirical spatial patterns of disease spread could be observed.

In the model, it is assumed that measurements from different cities are available for each day (using interpolation of weekly data) during the course of the epidemic, with the exception of a few days with possible missed reports. For each simulation day, daily counts above a specified threshold are provided to the algorithm. In order to study the algorithm behavior in different scenarios, manual modification to daily numbers and the threshold were performed in some experiments, when needed.

The problem is then to perform estimation at each time step when new measurements are reported until the "cutoff" day, after which the goal is to predict the epidemic curve (which is the number of infected population through time). The prediction is performed using the estimated parameters of the SIR model in the state vector. The predictive performance of the proposed algorithm was compared with the "true" number of reported cases obtained from the dataset, and also with the result of a SIR curve fit obtained using an exhaustive search. The initial number of particles was set to 6000 consisting of $L_s = 5000$ for the survived and spawned targets and $L_b = 1000$ for new targets. The algorithm assumed partial knowledge of model parameters using $\beta \in [0.1, 0.9]$ and $\upsilon \in [0.1, 0.9]$. Disease transition probabilities were also selected based on real-world data such that transition Geneva to Lausanne and Lausanne to Bern has the highest probabilities assigned. More precise estimates of these parameters could be obtained from detailed epidemiological studies of an emerging epidemic. These estimates would then simply be incorporated into models such as the one here.

The dataset files and implementation sources files in MATLAB are available from https://prlab.um.ac.ir/index.php/resources/.

B. Prediction Performance

In the following set of results, prediction errors for the upcoming observations at each cutoff day during the course of the epidemic are calculated. The results are compared with the SIR fit over the observations using an exhaustive search. Regression and model fitting approaches are common in the biosurveillance literature for comparison and validation [7], [45].

Fig. 1 compares the prediction results of the model and SIR fit for different cutoff days. This figure serves to demonstrate the prediction robustness of the proposed algorithm by filtering out noisy data and incorporating prior knowledge into the model. Although the predefined intervals for parameters β and γ were the same, the fitted SIR curve suffers from imprecise predictions and high fluctuations, especially during the early days of monitoring.

C. Prior Knowledge in Early Prediction

As more observations become available, prior knowledge on partially known model parameters is increased. The possible similarity of epidemic waves (see Section II-B) would then help improve early prediction when a new population is infected.

Fig. 2 displays estimation and prediction results after ten days of monitoring the epidemic waves for selected cities. It is observed that the 95% confidence interval area gets tighter in the second and third wave. A subset of particles for Lausanne and Bern are generated based on current estimates in Geneva and Lausanne, respectively, using (15), which improves convergence for these cities. In the second and third waves, the particles are more concentrated in the vicinity of SIR fit.

Studying Fig. 2, one can make the observation that in accordance with our expectations, the estimation and prediction results are more certain when prior knowledge of parameters β and υ is gathered during the first wave. However, even when the knowledge of these parameters is imprecise, the reported cases corresponding to what we consider as the "true" number of infected people (empty diamonds) are always enveloped by predictions after a few days of monitoring.

D. Disease Transition Probabilities

Based on the prior knowledge of west–east direction of epidemic spread [26], [15], disease transition probabilities were selected such that the first wave of influenza epidemic is more probable to appear in Geneva. The epidemic would spread to Lausanne with high probability and from there to the next city, Bern. The following experiment studies the influence of the predefined disease transition probabilities on the proposed algorithm. In Fig. 3 the "true" observations for the first 40 days of monitoring, together with state estimate of infected population are displayed. The horizontal solid line is the event threshold, determining which observations are fed to the filtering algorithm.

Disease transition probabilities dictate the corresponding population system in the randomly generated state vectors. In this case, more state vectors for Geneva are generated.

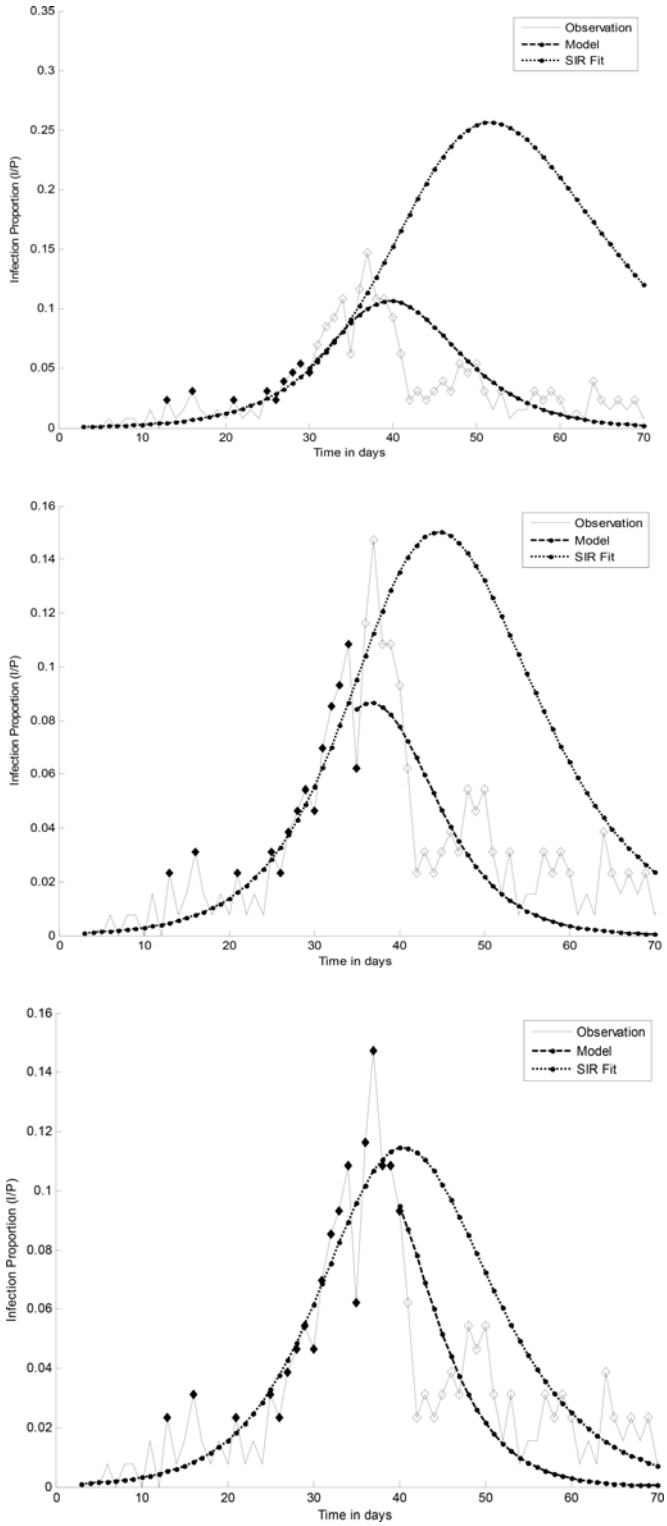

Fig. 1. Prediction results for day 30, 35, and 40 for Lausanne. The bold and thin dashed lines are the predicted curves for model and the SIR fit, respectively.

Since the set of the state vectors representing spontaneous epidemics Γ_k contains more particles for Geneva, on days 8 and 9 the (manually modified) number of reported cases are not detected as an ongoing epidemic and are ignored as false alarms simply because the summation of the corresponding particle

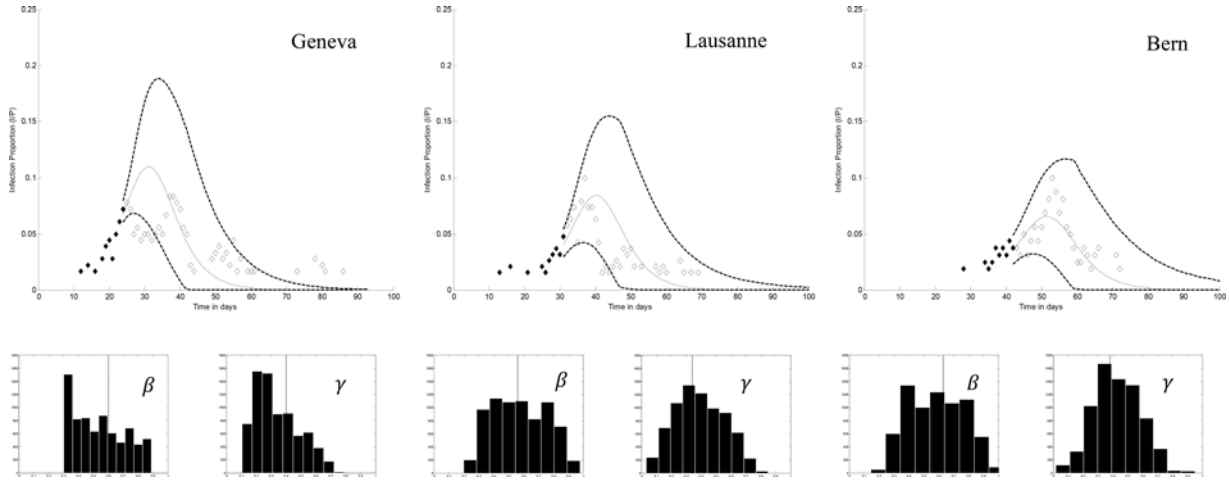

Fig. 2. Estimated epidemic curves and histograms of model parameters β and γ after ten days of monitoring in selected cities. Predicted curve and 95% confidence intervals are displayed by solid and dashed lines, respectively. In the histograms, the vertical dashed line is the result of SIR fit over all observations.

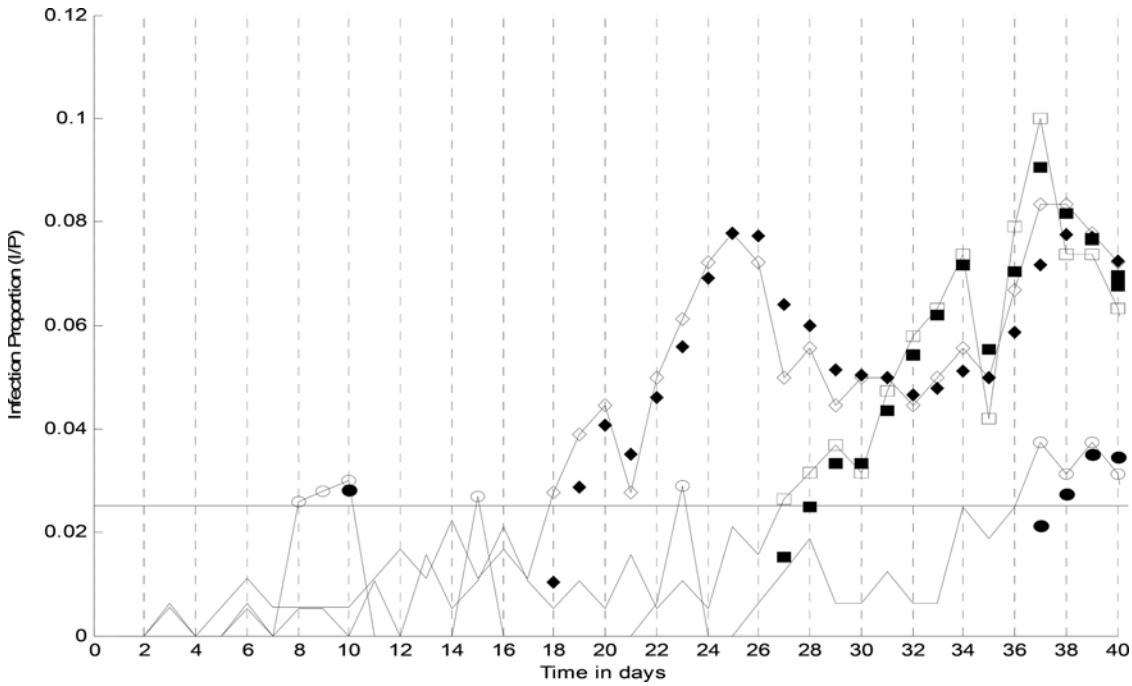

Fig. 3. Influence of epidemic transition probability in model behavior. Empty circles, diamonds and squares are "true" number of reported cases for Bern, Geneva, and Lausanne, respectively. The filled marks represent model estimated number of reported cases and the horizontal solid line is the threshold. The epidemic is expected to start in Geneva and from there spread to Lausanne and Bern.

weights (N_k) is not greater than 1, until the third report on day 10. Comparing with the algorithm behavior on day 18, a single report for Geneva is estimated as an epidemic and is tracked during the following days.

Once an ongoing epidemic is detected in a city, detection sensitivity is increased for its neighbors as more particles are generated, representing target birth through spatial spread with $B_{k|k-1}$ in (16). This is the case of the first report of Lausanne on day 26 and also the sixth report of Bern on day 36.

E. Spatial Information

In this section, the effects of spatial information in prediction results are studied. To this end, a comparison of the prediction accuracy and confidence of the proposed algorithm with a version of the algorithm with no spatial information (zero disease transition probability) and also a similar approach based on a single target (no spatial information) particle filter [16], is provided.

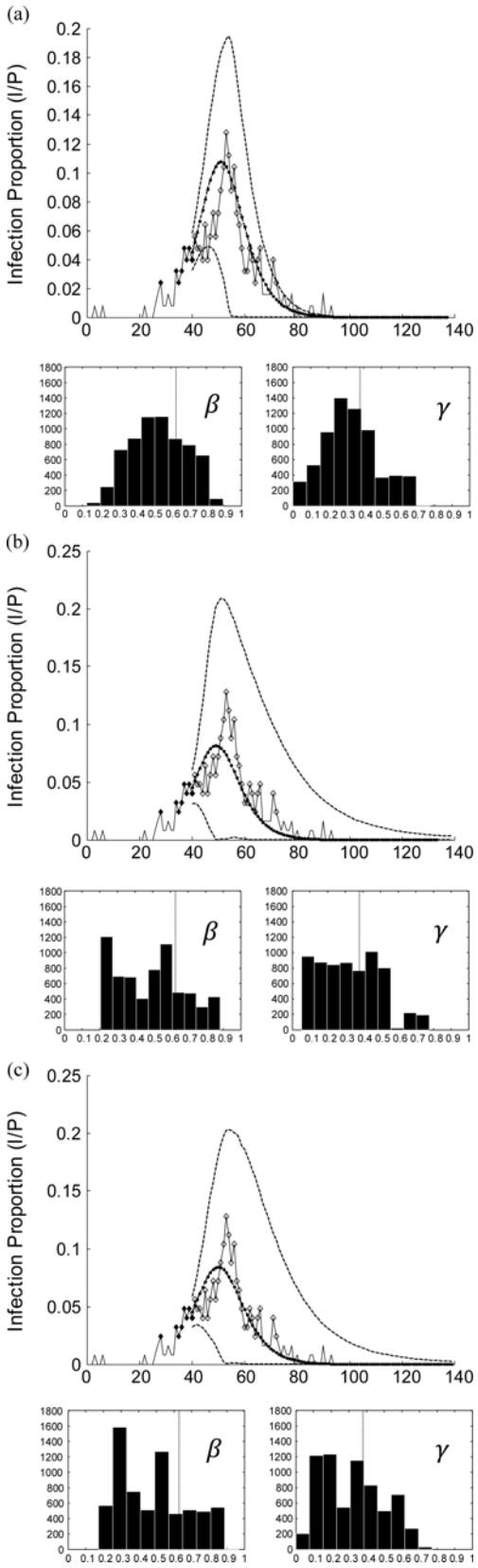

Fig. 4. Prediction results and confidence interval after 40 days of monitoring in city Bern; (a) proposed algorithm, (b) proposed algorithm with no spatial information provided and (c) single target particle filter implementation with no spatial information as in [16]. Marks and symbols as in Fig. 2.

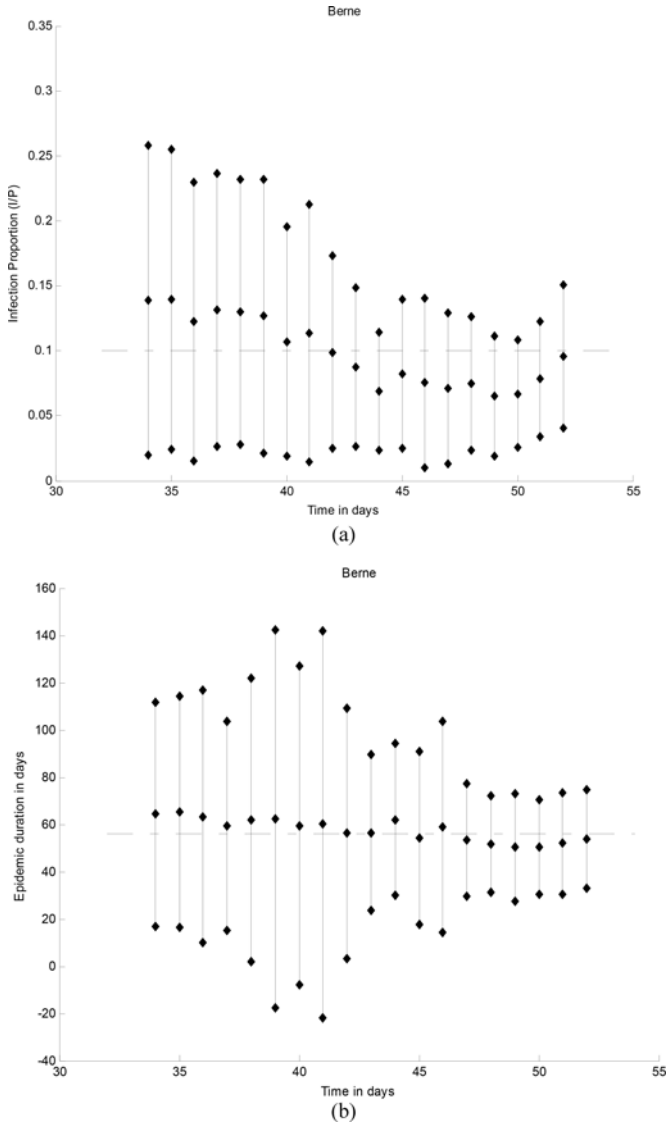

Fig. 5. (a) Epidemic peak intensity $i_{\max}$ and (b) duration d for cutoff days 34–52 in reported cases of city of Bern together with the confidence intervals. The results are averaged over ten runs of the algorithm. Parameter values obtained by fitting a SIR curve to data of the epidemic wave are shown with the horizontal line.

With disease transition probabilities defined beforehand, prior knowledge on SIR model parameters in form of range values are acquired during the monitoring phase. This improves the prediction results by providing a set of starting points in the search space of the problem for the newly infected areas.

As depicted in Fig. 4, the confidence interval is tighter and the predicted parameters are more concentrated around the "right" answer in the proposed algorithm as opposed to the other two methods.

By ignoring disease transition probabilities [see Fig. 4(b)], the prior knowledge on SIR model parameters is lost. It can be observed that the confidence margin in this case is larger and the histogram of predicted parameters display a wide range of possibilities. This is also true for any similar algorithm without this kind of prior knowledge as shown in Fig. 4(c).

F. Peak Duration and Intensity Prediction

Prediction performance of epidemic duration and peak intensity is studied in the final set of results (see Fig. 5). For the epidemic in Bern, $d = 56$ and $i_{\max} = 0.1$. At each cutoff day, intensity is computed using the approximate formulae from Theorem 2.1 in [46] under the assumption that initial susceptible population $s_0 \approx 1$ and initial infected population $i_0 \approx 0$.

$$i_{\max} \approx 1 - \rho^{-1} + \rho^{-1} \log(\rho^{-1}) \tag{27}$$

where $\rho = \frac{\beta}{\gamma}$ (see Section III-A). Parameters γ and β are estimated from the observations available up to the cutoff day (current estimate of the state vector). The duration of the epidemic is calculated by measuring the size of an SIR curve simulation using the estimated β and γ. The results further show that duration and intensity are reasonably acceptable, even in short periods of observation. The uncertainty in estimation decreases as more observations become available.

VI. Conclusion

In this paper, we proposed an algorithm for estimation and prediction of epidemic outbreaks formulated in the context of multitarget nonlinear filtering, based on the set of observations of the number of infected people in loosely coupled population systems. The epidemic progression in time is modeled using the classical compartmental SIR model. While an independent set of SIR parameters is used to model the epidemic dynamics within each area, the proposed framework is capable of modeling spatial information as well. This is carried out by defining a set of transition probabilities between each pair of monitored geographical areas. Prediction and estimation results for newly infected areas also benefit from early convergence by narrowing the range of possible model parameters based on epidemic behavior in neighboring areas. The algorithm, implemented as a particle-PHD filter, provides continuous estimation of the state of all epidemics, including the infected population and the partially known parameters of the SIR model for every population system. Experimental results show that the proposed framework can be useful in providing timely prediction of the epidemic peak and duration when the uncertainty in prior knowledge of model parameters is limited.

The proposed method is rather a conceptual solution for a new biosurveillance and still at its early stages of development. Further research is concerned with practical problems regarding its operational deployment. For instance, there is a potential challenge in selecting more complicated epidemic models and also incorporating population migration patterns (variable population). Our future work would involve a generalization of the proposed framework to include more realistic criterions with regards to known ecological and biological features of animal and human populations.

References

[1] Y. Le Strat and F. Carrat, "Monitoring epidemiologic surveillance data using hidden Markov models," *Stat. Med.*, vol. 18, no. 24, pp. 3463–3478, 1999.

[2] X. Jiang, G. Wallstrom, G. F. Cooper, and M. M. Wagner, "Bayesian prediction of an epidemic curve," *J. Biomed. Inform.*, vol. 42, no. 1, pp. 90–99, Feb. 2009.

[3] H. Liang and Y. Xue, "Investigating public health emergency response information system initiatives in China," *Int. J. Med. Inform.*, vol. 1, no. 2, p. 9–10, 2004.

[4] R. M. Anderson, C. Fraser, A. C. Ghani, C. a Donnelly, S. Riley, N. M. Ferguson, G. M. Leung, T. H. Lam, and A. J. Hedley, "Epidemiology, transmission dynamics and control of SARS: The 2002–2003 epidemic," *Philos. Trans. Roy. Soc. Lond. B., Biol. Sci.*, vol. 359, no. 1447, pp. 1091–1095, Jul. 2004.

[5] C. Robertson, T. A. Nelson, Y. C. Macnab, and A. B. Lawson, "Review of methods for space-time disease surveillance," *Spat. Spatiotemporal Epidemiol.*, vol. 1, no. 2–3, pp. 105–116, Jul. 2010.

[6] J. Manitz, "Automated detection of infectious disease outbreaks," Diploma thesis, Ludwig-Maximilians-Universität München, München, Germany, 2010.

[7] X. Zhou, Q. Li, Z. Zhu, H. Zhao, H. Tang, and Y. Feng, "Monitoring epidemic alert levels by analyzing internet search volume," *IEEE Trans. Biomed. Eng.*, vol. 60, no. 2, pp. 446–452, Feb. 2013.

[8] B. J. Paterson and D. N. Durrheim, "The remarkable adaptability of syndromic surveillance to meet public health needs," *J. Epidemiol. Global Health*, vol. 3, no. 1, pp. 41–47, 2013.

[9] W. H. Woodall, J. B. Marshall, M. D. Joner, and E. Shannon, "On the use and evaluation of prospective scan methods for health-related surveillance," *J. Roy. Statist. Soc., Ser. A*, vol. 171, pp. 223–237, 2008.

[10] C. Sonesson and D. Bock, "A review and discussion of prospective statistical surveillance in public health," *J. Roy. Statist. Soc., Ser. A*, vol. 166, no. 1, pp. 5–21, 2003.

[11] S. Straif-Bourgeois and R. Ratard, "Handbook of Epidemiology," in *Handbook of Epidemiology*. New York, NY, USA: Springer-Verlag, 2005, pp. 1328–1362.

[12] M. Wagner, A. Moore, and R. Aryel, *Handbook of Biosurveillance*. New York, NY, USA: Academic, 2006.

[13] D. D. L. Buckeridge, H. Burkom, M. Campbell, W. R. Hogan, and A. W. Moore, "Algorithms for rapid outbreak detection: A research synthesis," *J. Biomed. Inform.*, vol. 38, no. 2, pp. 99–113, 2005.

[14] A. Corberán-Vallet, "Prospective surveillance of multivariate spatial disease data," *Stat. Methods Med. Res.*, vol. 21, pp. 457–477, Apr. 2012.

[15] T. Smieszek, M. Balmer, J. Hattendorf, K. W. Axhausen, J. Zinsstag, and R. W. Scholz, "Reconstructing the 2003/2004 H3N2 influenza epidemic in Switzerland with a spatially explicit, individual-based model," *BMC Infect. Dis.*, vol. 11, no. 1, pp. 115–133, Jan. 2011.

[16] A. Skvortsov and B. Ristic, "Monitoring and prediction of an epidemic outbreak using syndromic observations," *Math. Biosci.*, vol. 240, no. 1, pp. 12–19, Nov. 2012.

[17] C. Jègat, F. Carrat, C. Lajaunie, and H. Wackernagel, "Early detection and assessment of epidemics by particle filtering," in *geoENV VI—Geostatistics for Environmental Applications*, vol. 15, A. Soares, M. Pereira, and R. Dimitrakopoulos, Eds. Dordrecht, Netherlands: Springer, 2008, pp. 23–35.

[18] B. Ristic, "Predicting the progress and the peak of an epidemic," in *Proc. IEEE Int. Conf. Acoustics, Speech Signal Process.*, 2009, pp. 513–516.

[19] I. Sazonov, M. Kelbert, and M. B. Gravenor, "The speed of epidemic waves in a one-dimensional lattice of SIR models," *Math. Model. Nat. Phenom.*, vol. 3, no. 4, pp. 28–47, Dec. 2008.

[20] D. J. Daley and J. Gani, *Epidemic Modelling: An Introduction*. Cambridge, U.K.: Cambridge Univ. Press, 2001.

[21] J. D. Murray, *Mathematical Biology*, 3rd ed. London, U.K.: Springer-Verlag, 1989.

[22] M. J. Keeling and L. Danon, "Mathematical modelling of infectious diseases," *Brit. Med. Bull.*, vol. 92, pp. 33–42, Jan. 2009.

[23] L. Rass and J. Radcliffe, "Spatial deterministic epidemics," *Bull. Amer. Math. Soc.*, vol. 42, no. 4, pp. 521–527, 2005.

[24] N. Ferguson, C. Donnelly, and R. Anderson, "Transmission intensity and impact of control policies on the foot and mouth epidemic in Great Britain," *Nature*, vol. 413, pp. 542–548, 2001.

[25] D. Mollison, *Epidemic Models: Their Structure and Relation to Data*. Cambridge, U.K.: Cambridge Univ. Press, 1995.

[26] J. Paget and R. Marquet, "Influenza activity in Europe during eight seasons (1999–2007): An evaluation of the indicators used to measure activity and an assessment of the timing, length and course of peak activity (spread) across Europe," *BMC Infect. Dis.*, vol. 30, no. 7, pp. 141–148, 2007.

[27] D. L. Smith, B. Lucey, L. A. Waller, J. E. Childs, and L. A. Real, "Predicting the spatial dynamics of rabies epidemics on heterogeneous landscapes," *Proc. Nat. Acad. Sci. USA*, vol. 99, no. 6, pp. 3668–72, Mar. 2002.
[28] S. S. Lee and N. S. Wong, "Reconstruction of epidemic curves for pandemic influenza A (H1N1) 2009 at city and sub-city levels," *Virol. J.*, vol. 7, no. 1, pp. 321–327, Jan. 2010.
[29] I. M. Hall, R. Gani, H. E. Hughes, and S. Leach, "Real-time epidemic forecasting for pandemic influenza," *Epidemiol. Infect.*, vol. 135, no. 3, pp. 372–385, Apr. 2007.
[30] A Flahault, S Letrait, P. Blin, S. Hazout, J. Ménarés, and A. J. Valleron, "Modelling the 1985 influenza epidemic in France," *Stat. Med.*, vol. 7, pp. 1147–1155, 1988.
[31] R. Anderson and R. May, "Population biology of infectious diseases: Part I," *Nature*, vol. 280, pp. 361–367, 1979.
[32] B. Deal, C. Farello, M. Lancaster, T. Kompare, and B. Hannon, "A dynamic model of the spatial spread of an infectious disease: the case of fox rabies in Illinois," *Environ. Model. Assessment*, vol. 5, pp. 47–62, 2000.
[33] W. Plowright, "Research on wildlife diseases: Is a reappraisal necessary?" *Revue Scientifique et Technique de l'OIE*, vol. 7, no. 4, pp. 783–795, 1988.
[34] R. Mahler, "The random set approach to data fusion," *Proc. SPIE*, vol. 2234, pp. 287–295, 1994.
[35] R. Mahler, "Multitarget Bayes filtering via first-order multitarget moments," *IEEE Trans. Aerosp. Electron. Syst.*, vol. 39, no. 4, pp. 1152–1178, Oct. 2003.
[36] I. Goodman, R. Mahler, and H. Nguyen, *Mathematics of Data Fusion*. New York, NY, USA: Springer, 1997.
[37] R. Mahler, "Global integrated data fusion," presented at the 7th Nat. Symp. Sens. Fusion, Albuquerque, NM, USA, 1994.
[38] B. Vo, S. Singh, and A. Doucet, "Sequential Monte Carlo methods for multitarget filtering with random finite sets," *IEEE Trans. Aerosp. Electron. Syst.*, vol. 41, no. 4, pp. 1224–1245, Oct. 2005.
[39] B.-N. Vo and W.-K. Ma, "The Gaussian mixture probability hypothesis density filter," *IEEE Trans. Signal Process.*, vol. 54, no. 11, pp. 4091–4104, Nov. 2006.
[40] D. Clark, "Multiple target tracking with the probability hypothesis density filter," Ph. D. thesis, Heriot-Watt University, Riccarton, U.K., 2006.
[41] R. P. Mahler, "A theoretical foundation for the Stein–Winter probability hypothesis density (PHD) multi-target tracking approach," presented at the MSS Nat. Symp. Sensor Data Fusion, San Antonio, TX, USA, 2000.
[42] A. S. Stordal, "Sequential Monte Carlo methods for Bayesian filtering," Ph.D. thesis, University of Bergen, Bergen, Norway, 2008.
[43] H. Sidenbladh, "Multi-target particle filtering for the probability hypothesis density," in *Proc. 6th Int. Conf. Inform. Fusion*, 2003, pp. 800–806.
[44] T. Zajic and R. Mahler, "Particle-systems implementation of the PHD multitarget-tracking filter," *Proc. SPIE*, vol. 5096, pp. 291–299, 2003.
[45] R. Vullings, B. de Vries, and J. W. M. Bergmans, "An adaptive Kalman filter for ECG signal enhancement," *IEEE Trans. Biomed. Eng.*, vol. 58, no. 4, pp. 1094–1103, Apr. 2011.
[46] H. Hethcote, "The mathematics of infectious diseases," *SIAM Rev.*, vol. 42, no. 4, pp. 599–653, 2000.

Amin Zamiri was born in Tehran, Iran, in 1985. He received the B.S. degree from the Ferdowsi University of Mashhad, Mashhad, Iran and the M.S. degree in software engineering from Shahid Beheshti University, Tehran, Iran, in 2010.

He is currently a researcher at Ferdowsi University of Mashhad. His research interests include multisource multitarget information fusion, data mining and artificial intelligence.

Hadi Sadoghi Yazdi received the B.S. degree in electrical engineering from Ferdowsi Mashad University of Iran, in 1994, the M.Sc. and the Ph.D. degrees in electrical engineering from Tarbiat Modarres University of Iran, Tehran, in 1996 and 2005, respectively. He works in Department of Computer Engineering as Associate Professor at Ferdowsi University of Mashhad. His research interests include pattern recognition, and optimization in signal processing. He has more than 40 journal publications in the areas of interest.

Sepideh Afkhami Goli received her B.S. degree from Ferdowsi University of Mashhad, Iran and M.S. degree in Information Technology from Sharif University, Tehran, Iran.

She is currently working towards Ph.D. degree at Calgary University, Alberta, Canada, focusing on multisource multitarget information fusion, data mining and artificial intelligence with applications in cooperative intelligent transportation systems.